Crystal-field splittings and magnetic properties of Pr^{3+} and Nd^{3+} in $RBa_2Cu_3O_7$

L. Soderholm, C.-K. Loong, G. L. Goodman, and B. D. Dabrowski
Argonne National Laboratory, Argonne, Illinois 60439
(Received 6 June 1990; revised manuscript received 24 October 1990)

Neutron inelastic scattering spectra are reported for superconducting $NdBa_2Cu_3O_7$ and insulating $PrBa_2Cu_3O_7$. These spectra are analyzed in terms of standard crystal-field theory for 3+ rare-earth ions in a manner that is consistent with the level assignments made in a similar study of $HoBa_2Cu_3O_7$. Using the eigenfunctions and eigenvalues obtained from this analysis of the inelastic neutron scattering spectra, the corresponding magnetic susceptibilities as a function of temperature were calculated according to the van Vleck formalism. Good agreement with experimental susceptibilities is achieved for all three compounds over the range of 100 to 300 K. The observed magnetic scattering in $NdBa_2Cu_3O_7$ agrees very well with the crystal-field calculations. In spite of the observed large intrinsic widths of the experimental crystal-field peaks for $PrBa_2Cu_3O_7$, the measured intensity is consistent with the calculated crystal-field excitation spectrum for Pr^{3+} ions in this lattice. The standard crystal-field treatment of Pr^{3+} ions is shown to explain the magnetic properties of $PrBa_2Cu_3O_7$ with no need to consider either the static or dynamic coexistence of Pr^{3+} and Pr^{4+}.

INTRODUCTION

Compounds of the type $RBa_2Cu_3O_7$ (abbreviated R-1:2:3-O_7) form an important family of superconducting materials with critical temperatures (T_c's) near 92 K.[1-3] Here R can be Y, Cm, or any rare earth except Ce, Pr, or Tb. Ce and Tb do not replace Y to form a single phase material, Pr-1:2:3:-O_7, on the other hand, does form, and is an isostructural member of the R-1:2:3-O_7 series, but is still not superconducting.[4] Indeed, Pr-1:2:3:-O_7 is not even metallic.[4,5] Furthermore, the Pr moments order antiferromagnetically with a Néel temperature (T_N) of 17 K.[6,7] This is in contrast to the other R-1:2:3:-O_7 compounds, in which the rare-earth moments order at much lower (<2.5 K) temperatures.[8,9] Recently, we have used the actinide curium ($Z=96$), to prepare and characterize Cm-1:2:3-O_7, showing it to be a second nonsuperconducting member of the orthorhombic Y-1:2:3-O_7 series.[10] The temperature dependence of the magnetic susceptibility indicates that the Cm moments order at 22 K.

The unique behavior of Pr-1:2:3:-O_7 and Cm-1:2:3-O_7 is not likely to arise from structure-related factors because both compounds are isostructural with the superconducting members of the R-1:2:3-O_7 series. Instead, we believe that unusual features in the electronic properties of the f-electron elements, Pr and Cm, are responsible for suppressing superconductivity in these materials. To investigate this hypothesis we have probed the low-energy electronic states of Pr in Pr-1:2:3-O_7 by a combination of inelastic neutron scattering and magnetic susceptibility measurements. Sample size requirements have prohibited a similar experiment on our sample of the analogous Cm compound. Instead, we compare and contrast our results with those obtained from Nd in Nd-1:2:3-O_7, a 92-K superconductor.[11]

Although several specific mechanisms have been suggested to account for the special behavior of Pr-1:2:3:-O_7, no comprehensive, generally accepted picture has yet emerged. Two basically different points of view have been proposed to account for the absence of a superconducting transition in Pr-1:2:3-O_7. From one point of view, Pr is argued to be a "mixed valent" ion in this material, with an average value of 3.5+ or higher.[12-18] The electrons that are regarded as oxidized away from a normal trivalent Pr^{3+} ion are thought to fill hole states in the conduction band and thereby to inhibit any superconducting transition. From the second point of view, Pr is argued to be a trivalent ion with a normal open-shell f^2-configuration.[5,19-23] In this case the interactions between the f electrons of the Pr^{3+} ion and the conduction electrons are thought to be strong enough to inhibit any superconductivity. It can be argued that each of these postulated mechanisms should be particularly favored for Pr and Cm, as compared to the other lanthanides, and that either mechanism would be sufficient to prevent the onset of superconductivity.

The main argument used in favor of a "mixed-valent" system comes from interpretation of magnetic susceptibility data for Pr-1:2:3-O_7. The effective moment, determined from the temperature dependence of the susceptibility, is about 2.8 Bohr magnetons (abbreviated μ_B).[12-19] This observed value is intermediate between that expected for a Pr^{3+} free ion ($3.58\mu_B$) and that for a Pr^{4+} fee ion ($2.54\mu_B$). Thus, it is said that the observed effective moment indicates a "mixed valence" for the Pr ion. In this context "mixed valence" for the Pr ion means that the average electronic occupancy of the f shell is nonintegral and substantially smaller than two. As an added complication, the ground-state ordered, saturation moment, determined by neutron diffraction stud-

ies[7] on the magnetically ordered state, is found to be $(0.74\pm0.08)\mu_B$. This saturation moment can be compared with the $0.43\mu_B$ moment that is expected for a $|\pm1/2\rangle$ doublet, assuming this to be the crystal-field-split ground state for the $^2F_{5/2}$ term of a Pr^{4+} ion. A Pr^{3+} ion is expected to have a nondegenerate ground state due to the low symmetry of the Pr sites and therefore no ordered moment. In other words, the ordered saturation moment is larger than might be expected for either a Pr^{3+} or a Pr^{4+} ion in this site symmetry. No crystal-field level structure has yet been obtained directly from experiments for Pr-1:2:3-O_7.

Examining only the magnetic data, mixed-valent behavior appears to offer a plausible explanation for the absence of superconductivity in the Pr (and Cm) compounds, since Pr (and Cm) can be readily oxidized to the tetravalent state. Moreover, an *in situ* oxidation of Pr^{3+} should result in a corresponding reduction of Cu, and seems therefore analogous to what occurs when oxygen is removed from Y-1:2:3-O_7.[24,25] On the other hand, structural data,[19,26] such as trends in bond lengths and lattice constants, chemical stability ranges,[19] absorption spectroscopies,[20–22] and band-structure calculations,[27] all are consistent with essentially Pr^{3+}. Experimental evidence for the postulated interaction between Pr^{3+} spins and the conduction electrons comes from the broadened magnetic excitations observed by inelastic neutron scattering,[28] the anomalously large electronic specific heat,[17] the large magnetic ordering temperatures of Pr-1:2:3-O_7 and Cm-1:2:3-O_7 (Refs. 7 and 10) and also from the temperature dependence of the curvature of H_{c2} in the $(Y_{1-x}Pr_x)Ba_2Cu_3O_7$ series as a function of x.[5] However, the presence of essentially trivalent Pr requires some less obvious interaction with the charge carriers of the copper-oxygen system in order to explain the lack of superconductivity.

To further the understanding of some of the less obvious features of the electronic structure of these materials, we have performed a series of spin-polarized, local-density, cluster calculations on R-1:2:3-O_7 (R =Ho, Nd, Pr, and Cm).[29] In order to improve the reliability of the calculated charge and spin densities obtained in these calculations, we used the recently developed concept of chemically complete atoms embedded in an extended crystal lattice.[30] The Mulliken population analysis of spin-polarized molecular orbitals shows a similar effective charge on the four f elements. Since both Ho and Nd are expected to be trivalent, Pr and Cm are concluded to be trivalent as well. These molecular orbital studies show that Ho^{3+} and Nd^{3+} have the well-localized, essentially noninteracting f electrons, usually expected for lathanide ions. However, for Pr^{3+} and Cm^{3+}, the calculated molecular orbitals indicate some admixture of the f orbitals with Cu d orbitals. This admixture seems to indicate a possible mechanism by which the magnetic states of the f element can interact with the spin moments of the conduction-electron system. It should be stressed that, while there is some evidence of orbital admixture, there is no evidence of significant charge transfer. Although the molecular-orbital calculations reliably indicate overall charge distributions, they are not configured for the purpose of determining crystal-field splittings or magnetic moments for the f^n configuration.

The electronic behaviors of Pr^{3+} and Pr^{4+} are expected to be dissimilar, and established trends in well-behaved, isolated trivalent lathanide-ions are well documented.[31] Therefore we have set out to obtain further information about the low-lying energy states of the rare earths in these compounds by acquiring and analyzing inelastic neutron scattering and magnetic susceptibility data. Neutron scattering is particularly effective in probing the properties of low-energy states that are coupled by appreciable magnetic transitions. In this paper we interpret our neutron scattering results for Pr-1:2:3-O_7 and Nd-1:2:3-O_7 in terms of standard crystal-field analyses. Based on a published analysis for the analogous Ho compound,[32,33] we obtained crystal-field parameter sets for Pr^{3+} and Nd^{3+} which permit a consistent assignment of neutron scattering data. The same crystal-field parameters are used to calculate magnetic susceptibilities for Ho^{3+}, Nd^{3+}, and Pr^{3+} in R-1:2:3-O_7. These calculated susceptibilities are compared to corresponding experimental data. In this way we show quantitatively that standard crystal-field-splitting effects can fully explain the unusual bulk susceptibility observed for Pr-1:2:3-O_7.

EXPERIMENTS

Approximately 50 g of polycrystalline Nd-1:2:3-O_7 and (Pr_xY_{1-x})1:2:3-O_7 ($x=1$, 0.6, 0.4, 0.1, 0) and a 5-g sample of Ho-1:2:3-O_7 were prepared by standard solid-state techniques.[19] The samples were characterized by x-ray and, for the Nd and Pr samples, by neutron diffraction. The x-ray diffraction data were obtained using a Scintag θ-θ diffractometer, calibrated with a silicon standard. Neutron diffraction data were obtained using the GPPD powder diffractometer of the Intense Pulsed Neutron Source (IPNS), Argonne National Laboratory, and analyzed by standard Rietveld techniques.[34] All compounds were found to be isostructural with orthorhombic ($Pmmm$) Y-1:2:3-O_7.[35] No impurity phases were observed to within the experimental uncertainty for any of the samples.

Neutron inelastic scattering experiments were performed on about 40-g samples of polycrystalline $(Pr_xY_{1-x})Ba_2Cu_3O_7$ ($x=1$, 0.4, 0.1, and 0) and $NbBa_2Cu_3O_7$ using both the HRMECS and LRMECS chopper spectrometers, also at IPNS. These time-of-flight neutron spectrometers are equipped with wide-angle multidetector banks and thus enable measurements of inelastic scattering over a wide range of momentum and energy transfers ($\hbar Q,E$). In general, the energy resolution (FWHM), varies with energy transfer but is approximately 5–8% of the incident energy E_0 for LRMECS and 2–4% for HRMECS. To fully explore the crystal-field spectra up to 200 meV with good resolution, three incident energies, 40 and 250 meV on HRMECS, and 120 meV on LRMECS, were chosen for the studies. Measurements of the elastic incoherent scattering from a vanadium standard at each energy provided detector calibration and intensity normalization.

Polycrystalline samples, contained in an aluminum cell

shaped as a thin slab, were mounted either perpendicular or at a 45° angle to the incident beam. Such geometry limits the neutron path length traversing the material to less than 0.5 cm for all detector angles (3°–120°), thereby reducing multiple scattering of neutrons in the sample. The effective transmission for all samples was 90–95%. A container run at each energy was used to correct for background scattering. The experiments were performed at selective temperatures ranging from 4 to 300 K, using either a closed-cycle helium refrigerator or a conventional helium cryostat for sample cooling.

Since neutrons are scattered by (magnetic) electrons as well as by nuclei in the sample, a reliable extraction of the magnetic scattering from the observed intensity is very important for the interpretation of the data. This is accomplished in two ways. First, since Y has no magnetic electrons, the spectra of $YBa_2Cu_3O_7$ measured under identical experimental conditions were used to estimate the contributions from nuclear elastic and phonon scattering. While the phonon spectrum of Y-1:2:3-O_7 is expected to resemble those of the other R-1:2:3-O_7 spectra, there is evidence of important differences in the energy region between 25 and 40 meV, where contributions from lattice vibrations involving the Y (or R) atoms is significant. A second method useful in the identification of the scattering as magnetic in origin stems from the Q dependence of the scattering intensity. Neutron intensity from magnetic scattering by electrons is modulated by the square of the magnetic form factor, $|f(Q)|^2$, where $f(Q)$ is the Fourier transform of the spatial distribution of the electronic spin density. Magnetic scattering falls off rapidly with increasing Q as a result of the finite spatial extent of the f orbitals whereas intensity from one-phonon scattering increases with Q^2. Consequently, for each measured spectrum, nuclear (mainly phonon) scattering can be assessed from the data obtained at large Q ($Q \geq 8$ Å^{-1}). These two methods provide a means for the assignment of the crystal-field peak positions and intensities, and a consistency check of the overall results. Nevertheless, for data obtained from $(Pr_xY_{1-x})Ba_2Cu_3O_7$ samples, where the crystal-field peaks are broad and weak, we estimate a relatively large uncertainty (up to 20%) in the extracted magnetic intensities.

Magnetic susceptibility data were collected on a George Associates modified Faraday magnetometer over the temperature range $77 < T < 300$ K.

RESULTS

The neutron inelastic spectra obtained on Nd-1:2:3-O_7 (at 15 K, well below the superconducting critical temperature of 92 K) are shown in Fig. 1. Well-defined, sharp crystal-field peaks are observed at 12, 20.8, 36, and 117 meV. The peak energies agree well with those previously reported for Nd-1:2:3-O_7.[36,37] There are no additional peaks observed up to about 200 meV. The peaks seen at temperatures below the superconducting critical temperature (T_c) for Nd-1:2:3-O_7 are only slightly wider than the instrument resolution. However, the temperature dependence of the 20.8-meV peak width is unusually strong above T_c, and suggests some coupling of crystal-

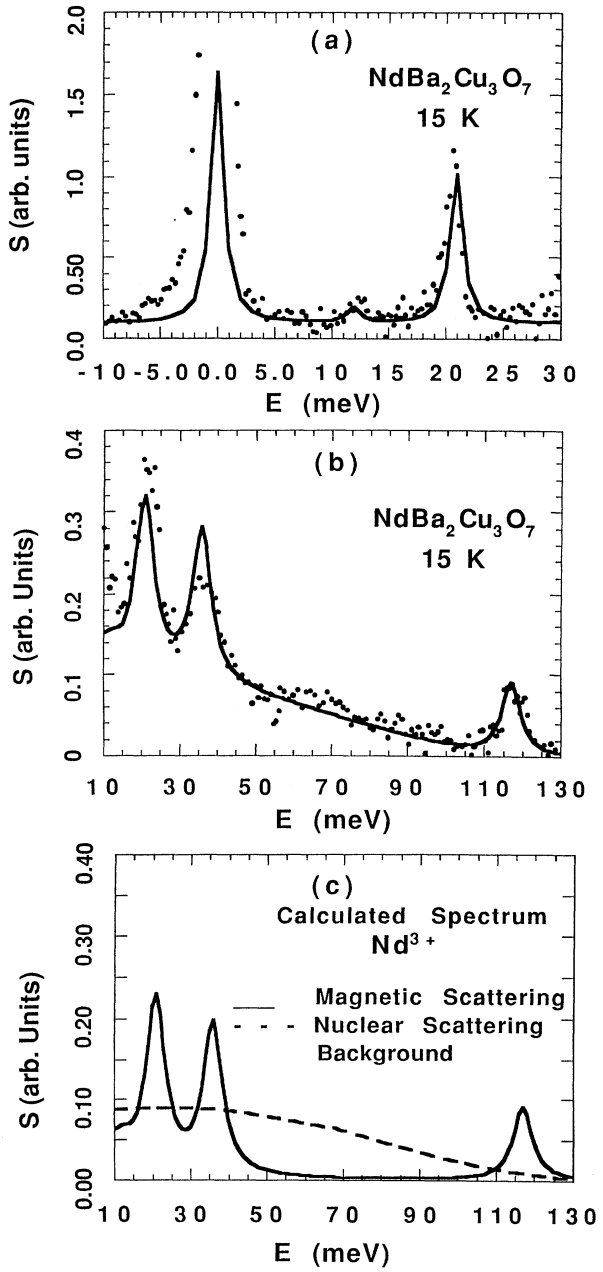

FIG. 1. Measured scattering functions for $NdBa_2Cu_3O_7$ at 15 K. (a) solid circles represent data obtained from HRMECS with $E_0 = 40$ meV. Magnetic peaks are observed at 12 meV ($Q = 1.18$ Å^{-1}) and 20 meV ($Q = 1.62$ Å^{-1}). The solid line is the spectrum calculated from the energy levels in Table III, which were obtained from the crystal-field parameters listed in Table I. The model spectrum was calculated with an assumed Lorentzian linewidth (at half length) of 1.3 meV. A constant background (0.09) has been added to the calculated spectrum. In panel (b), the solid circles represent data obtained from LRMECS ($E \leq 60$ meV) with $E_0 = 120$ meV and from HRMECS ($E \geq 60$) with $E_0 = 250$ meV. The solid line is the calculated spectrum, which is composed of the magnetic scattering and the background as shown individually in panel (c). A Lorentzian linewidth of 6.15 meV was used in the model spectrum. The Q dependence of the Nd^{3+} form factor has not been taken into account in the model spectra.

field states with the states involved in superconductivity.[38]

We have measured the magnetic excitation spectra of Y-1:2:3-O_7 at 15 K, Pr-1:2:3-O_7 at 4, 15, 25, and 100 K, as well as $Pr_{0.1}Y_{0.9}Ba_2Cu_3O_7$ ($T_c \approx 85$ K) and $Pr_{0.4}Y_{0.6}Ba_2Cu_3O_7$ ($T_c \approx 40$ K) at 15 and 100 K. The experimental data, after normalization according to Pr concentration, and correction for Bose temperature factors, are all very similar to those of Pr-1:2:3-O_7 at 15 K, which are shown in Fig. 2, together with the Y-1:2:3-O_7 data as a nonmagnetic background. To within experimental precision we find no evidence of significant difference between the 25- and 15-K spectra resulting from the antiferromagnetic ordering of the Pr moments.

The most notable feature of the data is the lack of any well-defined, sharp peaks in the Pr-1:2:3-O_7 spectra. Instead we see an intense, broad component of magnetic excitation from about 2 to about 15 meV and much weaker, broadened features at about 35, 45, 50, 65, 80, and 105 meV. (The 105-meV peak is obtained from a run on HRMECS with incident neutron energy of 250 meV, which is not shown.) According to a brief, preliminary report, a neutron experiment on Pr-1:2:3-O_7 performed at ISIS (Ref. 39) revealed similar results. While the features at energies above 40 meV are crystal-field excitations, we find that the structure in the region around 35 meV is due to phonon scattering, as indicated by its persistent intensity at high momentum transfer Q.

The bulk magnetic susceptibility, χ, measured for Pr-1:2:3-O_7 is plotted as χ versus $1/T$ over the temperature range 100 to 300 K, as shown in Fig. 3. The experimental susceptibility data have been fitted to the Curie-Law expression

$$\chi = \frac{C}{T} + \chi_0 ,$$

where χ_0 is the temperature independent susceptibility.

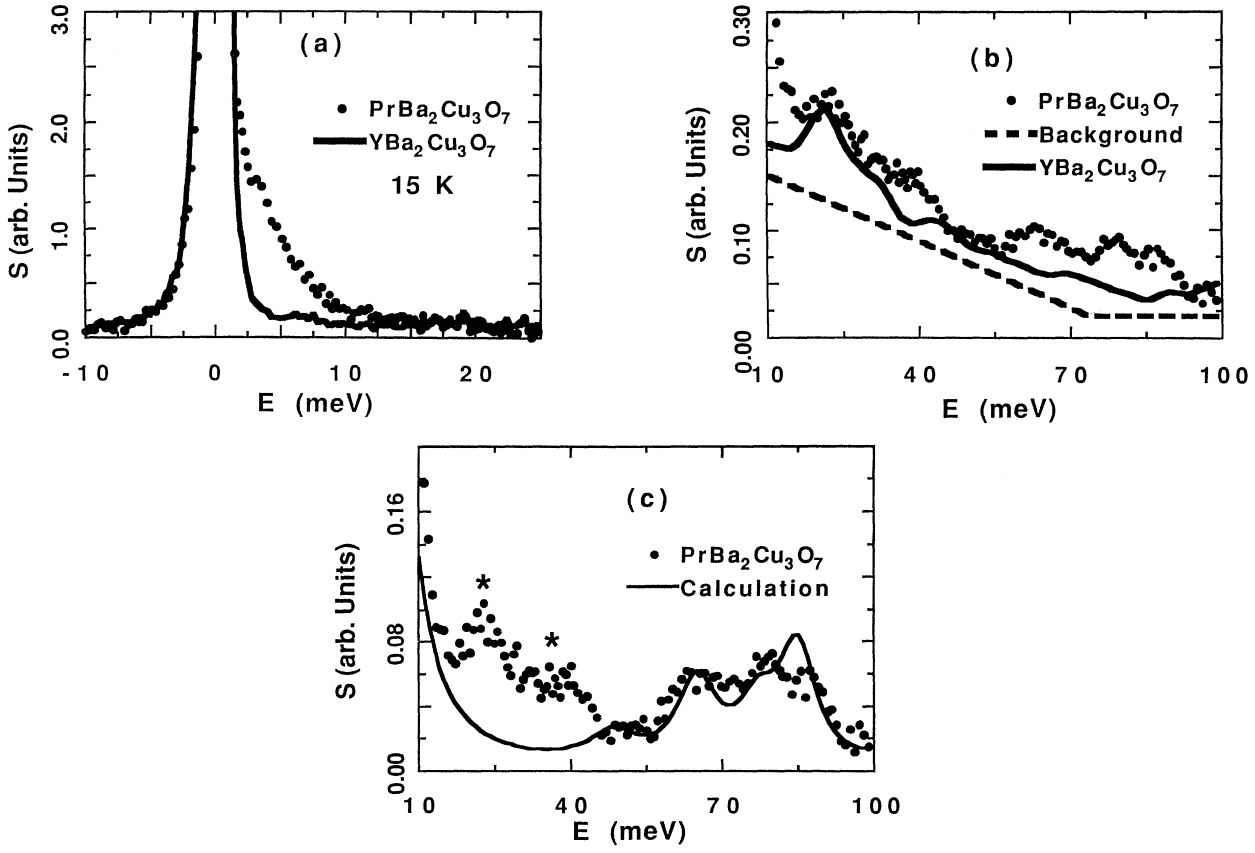

FIG. 2. (a) A comparison of Pr-1:2:3-O_7 data (circles) and Y-1:2:3-O_7 data (solid line) taken under similar conditions. The excess Pr scattering at low energy is magnetic in origin. Our analysis indicates that there are three unresolved crystal-field transitions at low energy. A more detailed analysis of the low-energy data ($0 \leq E \leq 20$ meV) is given elsewhere (Ref. 45). (b) Pr-1:2:3-O_7 data (circles) compared with Y-1:2:3-O_7 data (solid line) obtained at 15 K, from LRMECS with $E_0 = 120$ meV. These spectra are compared with the linear background (dashed line) subtracted from the data to obtain the circles in 2(c). It can be clearly seen that the background correction underestimates the nonmagnetic contribution at $E \leq 40$ meV. (c) Pr-1:2:3-O_7 data (circles) obtained from LRMECS with $E_0 = 120$ meV, after the removal of the background, shown in (b). The neutron wave vector Q, varies from about 2 at 0 meV, to 5 Å^{-1} at 100 meV. The solid line is the model spectrum, calculated for 15 K from the energy levels and magnetic strengths reported in Table IV by assuming a Lorentzian linewidth (at half height) of 9 meV. The Q dependence of the Pr^{3+} form factor has been taken into account for the calculated spectrum. The large excess in experimental intensity in the range $10 \leq E \leq 40$ meV (represented by the *) is nonmagnetic.

The Curie constant C is used to define an effective moment in terms of the Boltzmann constant k and Avogadro's number N as

$$\mu_{\text{eff}} \equiv (3kC/N\beta^2)^{1/2} ,$$

where β is the conversion factor to units of Bohr magnetons (μ_B). In this way observed values of $\mu_{\text{eff}}=2.84\mu_B$ and $\chi_0=2.18\times10^{-3}$ emu/mol have been obtained for Pr-1:2:3-O_7. The effective moment obtained here is similar to those reported elsewhere for this compound.[12–19]

The temperature dependence of the magnetic susceptibility of Ho-1:2:3-O_7 have also been measured. The Curie Law fits the data well, yielding an effective moment of $10.3\mu_B$. This observed value is near the free-ion moment of $10.61\mu_B$, and is also in agreement with other published values.[40]

CRYSTAL-FIELD ANALYSIS

The method used here for calculating the energy levels and magnetic properties of the $4f^n$ configuration in a crystalline environment is based on the computer programs developed by Crosswhite and Crosswhite,[41] and applied by Carnall *et al.*[42] The total Hamiltonian consists of two parts

$$H = H_{\text{FI}} + H_{\text{CF}} .$$

Here H_{FI} is the free-ion part, which includes the spherically symmetric one-electron term of the Hamiltonian, the electrostatic interaction between equivalent f electrons, the spin-orbit interaction, and a term accounting for higher-order corrections.[42] H_{CF} is the crystal-field term, which takes into account the effect of the electrostatic interaction arising from the surrounding ions on the f electrons. It is assumed that H_{CF} for $4f$ electrons is small compared with H_{FI} so that it can be treated by perturbation theory. For a free ion, each state $|\alpha,J\rangle$ (where α represents the other relevant quantum numbers), is $(2J+1)$fold degenerate. In the presence of a crystalline electric field this degeneracy will be lifted according to the site symmetry of the rare-earth ion in the crystal lattice. In general, the crystal-field split states are linear combinations of the $|\alpha,J,M_J\rangle$ states and the degree of mixing depends on the strength of the crystalline electric field. In the weak-field approximation, which applies well to the rare-earth elements, the total angular momentum J

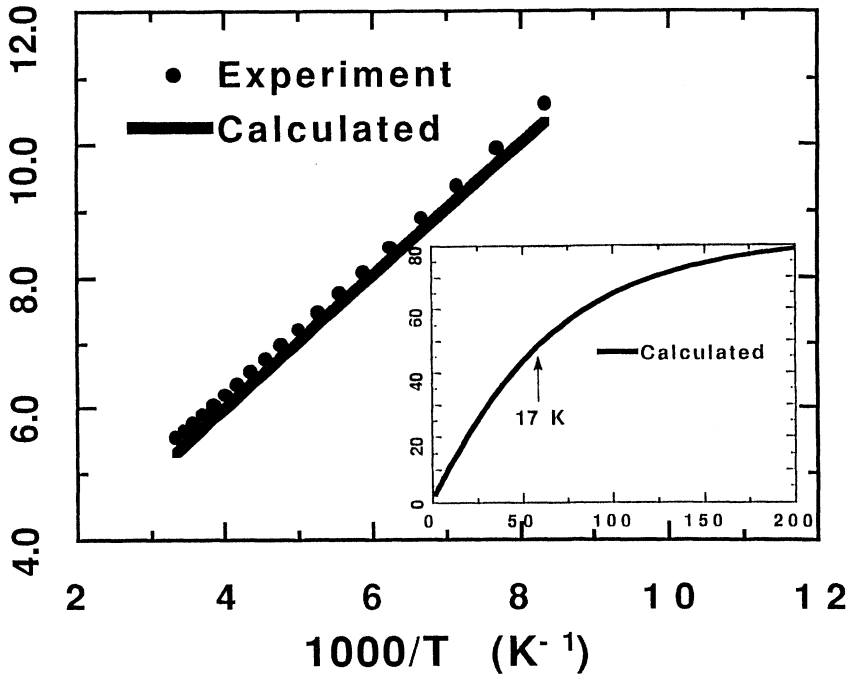

FIG. 3. The magnetic susceptibility of $PrBa_2Cu_3O_7$ plotted as χ vs $1/T$ over the temperature range 100–300 K. The slopes of the lines are proportional to the effective moments. As discussed in the text a temperature independent paramagnetic of $\Delta\chi_0=0.97\times10^{-3}$ emu/mol has been added to the susceptibility calculated for Pr^{3+} to represent the contribution to the overall susceptibility from the rest of the lattice. The inset shows the calculated susceptibility over a wider temperature range (5–600 K), to demonstrate the nonlinearity expected at lower temperature. The arrow indicates the 17-K onset temperature for the long-range ordering of the Pr moments in pure Pr-1:2:3-O_7. Below this ordering temperature we expect a significant renormalization of our calculated, single-site wave functions, as discussed in Ref. 45. Thus the calculated crystal-field susceptibility is only useful at low temperatures for dilute samples of $Y_{1-x}Pr_xBa_2Cu_3O_7$, which do not exhibit long-range magnetic ordering of the Pr moments.

of the f^n configuration remains a good quantum number. If the multiplets of different J's are well separated in energy compared to the intramultiplet splittings, the interactions between multiplets can be ignored. In such a case the crystal-field states can be calculated based solely on the ground-state splittings, using the Steven's operator equivalents method.[43] This computational simplification is often used for the rare-earth compounds. However, for the rare earths examined here, the crystal-field splittings within the Hund's rule ground term are about 100 meV. This splitting is comparable to the energy separation to the next J multiplet (approximately 200–500 meV for Pr, Nd, and Ho), and some intermultiplet interactions may be expected. Therefore a diagonalization of the full Hamiltonian using spherical tensor operator techniques under the scheme of intermediate coupling is more appropriate in these cases. This latter method takes into account possible interactions between states of different J multiplets. Conversion of the crystal-field parameters between these two methods has been worked out by Kassman[44] and other workers.

Our approach to the data analysis is to diagonalize the full Hamiltonian, including up to the 100 lowest-energy states of an f^n configuration. The free-ion states for the rare-earth ions are obtained from energy-level parameters for Ln^{3+}:LaF_3 given by Carnall *et al.*[42] The crystal-field part of the Hamiltonian is written as

$$H_{\mathrm{CF}}=\sum_{k,q,i} B_q^k C_q^k(i) \ , \tag{1}$$

where $C_q^k(i)$ is the qth component of a spherical tensor of rank k for the ith electron and

$$B_q^k=\langle r^k\rangle A_q^k \tag{2}$$

are the crystal-field parameters ($\langle r^k\rangle$ is a radial integral involving $4f$ radial wave functions). The formal expression of Eq. (2) does not warrant a factorization of $\langle r^k\rangle$ and A_q^k, however it does set an initial stage for a systematic treatment of the crystal-field parameters over the isostructural R-1:2:3-O_7 compounds, as will be discussed later.

The crystal-field site symmetry of the rare earth in the Y-1:2:3-O_7-type orthorhombic structure is *mmm* (D_{2h}).[35] A crystal field with this symmetry is characterized by nine real parameters. A site with this symmetry will, in principle, fully split the Pr^{3+} ground term ($4f^2$, $^3H_4$) into nine singlets, the Pr^{4+} ground term ($4f^1$, $^2F_{5/2}$) into three doublets, and the Nd^{3+} ground term ($4f^3$, $^4I_{9/2}$) into five doublets. Since there are seven transitions observed for Pr in Pr-1:2:3-O_7 above the Néel temperature we can immediately rule out an interpretation of these data based on Pr^{4+}, from which, in principle, only a maximum of three transitions (two from the ground state and one from the first excited state) would be expected.

The limited observations (eight levels for Pr and four levels for Nd) prevent the independent determination of all the crystal-field parameters. We have overcome this problem by using the level assignments for Ho-1:2:3-O_7, obtained from the detailed measurements of Furrer *et al.*,[32] as a starting point. These values were then rescaled to approximate the parameters expected for Nd^{3+} and Pr^{3+}, as outlined below, and discussed in detail elsewhere.[45]

Ho^{3+} was chosen as a reference because its ground-state term yields the largest number of crystal-field energy levels in the rare-earth series and because Ho-1:2:3-O_7 has previously been the subject of a careful, detailed study.[32] In a site with *mmm* symmetry, the ground term of Ho^{3+} ($4f^{10}$, $^5I_8$) should be completely split into 17 singlets. From inelastic neutron scattering data. Furrer *et al.* observed 10 crystal-field excitations. Using the energies of these excitations, together with their relative intensities, they were able to assign these observed excitation energies to specific transitions between calculated energy levels. Utilizing the Stevens formalism, they were able to obtain a full set of nine crystal-field parameters consistent with their data.

With slight adjustments of these parameters, under the irreducible tensor formalism, we were able to obtain a better fit to the Ho data,[32] but only minor changes in the relative values of the parameters. However, after extensive analysis of both the Ho and Pr data, we did find that a reassignment of the two energy levels, based on an analysis of the splittings resulting from a descent from cubic symmetry, improves the overall fit to all available data. The differences between the parameter sets and the assignments given by Furrer *et al.* and in this paper are probably within the experimental uncertainties of the observed transitions. The parameters are listed in Table I. For completeness, Table I also includes the crystal-field parameters obtained by Furrer *et al.*,[32] translated into the tensor convention. Listed in Table II are the corresponding energy levels together with our crystal-field symmetry assignments.

Having obtained good crystal-field parameters for Ho^{3+} in the R-1:2:3-O_7 lattice, we wish to scale these parameters to obtain corresponding values for Pr^{3+} and Nd^{3+} in the same environment. When scaling crystal-field parameters, there are two distinct factors which contribute to a change of parameter values: (1) variations in the external, electric field that arise from the crystal environment around the f element and (2) effects of the lanthanide contraction on spatial extent of the f-orbital wave functions. This change in the f-orbital wave function influences how sensitive f-electron energy levels are to their environment. There are only small changes in the lattice constants in passing from Ho-1:2:3-O_7 to Pr-1:2:3-O_7 (Refs. 19 and 40) and, as discussed below, molecular-orbital calculations indicate very little change in charge distributions for the rare-earth 1:2:3-O_7 compounds that we have studied.[29] Therefore, it is assumed that the external electric field is effectively constant for the cases of interest here.

Focusing on changes arising from the radial extent of the $4f$ wave functions, we attempted to use the classic Hartree-Fock radial averages $\langle r^k\rangle$'s for the appropriate Ln^{3+} (Ref. 46) to scale the crystal-field parameters. This procedure is known to overestimate the effects of the lanthanide contraction, and therefore it was also necessary to include an overall scaling correction. All the extrapolated crystal-field parameters were multiplied by a

TABLE I. Crystal-field parameters for Ho^{3+}, Nd^{3+}, and Pr^{3+} in R-1:2:3-O_7. All parameters are given in tensor formalism. The values of Furrer *et al.* (Ref. 32) (converted to the tensor notation) are included for completeness.

Crystal-field parameters	Ho^{3+} Ref. 32 (cm^{-1})	Ho^{3+} This work (cm^{-1})	Nd^{3+} this work (cm^{-1})	Pr^{3+} Scaled (cm^{-1})	Pr^{3+} Best fit (cm^{-1})
B_0^2	333.7	434.8	414.8[a]	440.3	449.36
B_0^4	−1763.2	−1907.5	−2640.3	−3015.9	−2785.2
B_0^6	448.8	471.6	603.8[a]	1067.0	808.4
B_2^2	59.27	76.6	179.0[a]	88.24	212.7
B_2^4	18.38	−297.4	−20.2[a]	50.62	15.27
B_4^4	972.7	1050.1	1698.1	1406.1	1498.0
B_2^6	−26.26	−252.6	−256.1[a]	−183.8	−325.4
B_4^6	1199.6	1305.1	1992.1	2792.8	2638.6
B_6^6	−12.4	−14.78	−3.76[a]	−4.79	−4.79[a]

[a]Fixed to the scaled value.

single adjustable rescaling factor to make the overall span of the calculated spectrum for Nd-1:2:3-O_7 agree with experiments. Details of this procedure are discussed elsewhere.[45]

Following a similar procedure, crystal-field parameters for Pr-1:2:3:-O_7 were extrapolated from combining the results of Ho^{3+} and the rescaling factor determined for Nd-1:2:3-O_7. While the energy levels obtained from these extrapolated parameters are somewhat different from those observed experimentally, they were close enough to allow assignments of the observed transitions. With eight energy transitions for Pr^{3+} we were able to obtain a fit for eight of the crystal field parameters. The data were very insensitive to the magnitude of B_6^6, which therefore was constrained to the value obtained from scaling of the Ho^{3+} value. These fitted Pr^{3+} parameters were then scaled to provide new Nd^{3+} parameters. Finally the three largest Nd^{3+} crystal field parameters, B_0^4, B_4^4, and B_4^6, were adjusted to fit the four observed transition energies, as reported in Tables I and III. The fitted assignments were checked by comparing calculated and experimental peak intensities, which agree well.

The observed and calculated scattering function for Nd-1:2:3-O_7 are shown in Figs. 1(a)–1(c). For unpolarized neutrons and polycrystalline samples, one measures a transition intensity proportional to $(2\mu_\perp+\mu_\parallel)/3$. The calculated crystal-field transitions for Nd^{3+} at 15 K, as shown by the solid curves in Figs. 1(a) and 1(c), were obtained by folding the calculated intensity with the appropriate instrumental resolution [Lorentzian functions with FWHM of 1.3 meV for Fig. 1(a) and 6.15 meV for Fig. 1(c)]. The crystal-field parameters obtained for Nd^{3+} are given in Table I and the corresponding observed and calculated energy levels are listed in Table III. The observed and calculated scattering function for Pr-1:2:3-O_7 at 15 K are shown in Fig. 2. The linewidth for the crystal-field peaks in the calculation is 9 meV for Fig. 2(c), significantly larger than the instrumental resolu-

TABLE II. The observed energy levels for Ho^{3+} in Ho-1:2:3-O_7, as reported by Furrer *et al.* (Ref. 32). These observed values are compared to the energies calculated by Furrer *et al.* and also to our calculated energies. The calculated energy levels are all nondegenerate, with the indicated symmetry classification (Γ) for our best fit. These assignments are discussed in detail elsewhere (Ref. 45).

Observed energies (Ref. 32) (meV)	Calculated energies Ref. 32 (meV)	Calculated energies This work (meV)	Our assignments Γ
0	0	0	3
0.5	0.13	0.81	2
1.8	1.28	2.11	4
3.8	3.60	3.74	1
4.3	3.81	4.31	3
8.1	7.61	8.34	1
10.8	10.28	11.31	2
11.6	10.75	12.01	4
	50.99	53.90	3
	51.44	56.62	1
59	53.42	58.83	4
59	53.54	59.32	2
	53.71	61.55	3
	57.00	62.82	1
70	62.81	69.05	2
	63.35	69.91	4
73	65.88	73.22	1

TABLE III. Observed energy levels for Nd-1:2:3-O_7. The calculated energies have been obtained from the crystal-field parameters listed in Table I. The energy levels are all doublets of Γ_5 symmetry.

Observed Energies Ref. 36 (meV)	Observed Energies Ref. 37 (meV)	This work (meV)	Calculated energies (meV)
0	0	0	0
12	12.6	12	12.2
20	21.5	20.8	20.4
36		36	36.2
		117	117.0

TABLE IV. The observed energy levels for Pr-1:2:3-O_7. They are compared to the energies obtained by scaling the Ho^{3+} crystal-field parameters, and also to the results of fitting, based on the scaled assignments. The calculated energy levels are all nondegenerate with the the indicated symmetry classifications Γ_n. Also included are the parallel and perpendicular transition strengths originating from the three lowest energy levels: A—the ground state, B—the first excited state, and C—the second excited state. These transition strengths are related to the expected intensity of the inelastic scattering lines, as discussed in the text.

Obs. (meV)	Energies Scaled (meV)	Fitted (meV)	Γ_n n	Magnetic Transition strengths (μ_B^2) $\lvert\mu_\parallel\rvert^2$	$\lvert\mu_\perp\rvert^2$	$\lvert\mu_\parallel\rvert^2$	$\lvert\mu_\perp\rvert^2$	$\lvert\mu_\parallel\rvert^2$	$\lvert\mu_\perp\rvert^2$
				A		B		C	
0	0	0	1	0	0	0	2.19	0	1.57
	0.2	1.5	2	0	2.19	0	0	4.42	0
4	3.7	4.1	4	0	1.57	4.42	0	0	0
45	44.4	45.1	1	0	0	0	0.09	0	0.15
50	53.2	50.3	3	0.18	0	0	0.32	0	0.64
65	66.8	65.1	2	0	0.54	0	0	0.71	0
80	76.4	80.0	4	0	0.38	0.47	0	0	0
85	85.3	85.1	3	1.80	0	0	0.36	0	0.25
105	110	104.9	1	0	0	0	0.51	0	0.70

tion. Transition energies for Pr^{3+}, together with their moments, are listed in Table IV. The Pr^{3+} crystal-field parameters obtained directly from scaling, together with those obtained from fitting are listed in Table I.

MAGNETIC SUSCEPTIBILITY

The determination of a consistent set of eigenfunctions and eigenvalues permits the calculation of the magnetic susceptibility of Ho^{3+}, Nd^{3+}, or Pr^{3+} in this crystal field. This is done here using the van Vleck formalism:[47,48]

$$\chi=\frac{N\mu_B^2}{3kTZ}\sum_{n,i}\left[\sum_j|\langle\phi_{n,i}|\boldsymbol{\mu}|\phi_{n,j}\rangle|^2 -2\sum_{j,m\neq n}\frac{|\langle\phi_{n,i}|\boldsymbol{\mu}|\phi_{m,j}\rangle|^2}{E_n-E_m}kT\right]\exp\left[-\frac{E_n}{kT}\right],$$

where $Z=\sum_n d_n\exp(-E_n/kT)$. Here ϕ_{ni} and ϕ_{nj} are the d_n degenerate eigenfunctions with energy E_n in the absence of a magnetic field. $\boldsymbol{\mu}$ is the magnetic moment operator $\boldsymbol{\mu}=(\mathbf{L}+2\mathbf{S})$. The first summation in the first set of large parentheses is over matrix elements diagonal in energy that normally produce Zeeman splitting in first-order perturbation theory. Usually these terms produce the dominant temperature-dependent contribution to the magnetic susceptibility, but in a low-symmetry site, for an ion with an even number of open-shell electrons like Ho^{3+} and Pr^{3+}, these first-order terms are all zero. The second summation inside the first set of large parentheses involves terms that arise in the second-order perturbation theory. In principle, these second-order terms would contribute only to the temperature-independent susceptibility, χ_0. But in cases like Ho-1:2:3:-O_7 or Pr-1:2:3-O_7, with nearly degenerate low-lying energy levels, these second-order terms can give rise to a temperature-dependent susceptibility for the intermediate temperature ranges under consideration here. When this type of complicated situation arises, the calculated susceptibility can be best treated the way an experimental susceptibility is normally treated, that is by fitting it to an empirical law. In this case the Curie Law is used to obtain an effective magnetic moment, μ_{eff}, and the corresponding χ_0 from the calculated susceptibility, for comparison with experiment.

This calculated magnetic susceptibility has been fit using the procedures outlined in the Results section. Fitted values of $\mu_{\text{eff}}=2.83\mu_B$ and $\chi_0=1.21\times10^{-3}$ emu/mol are obtained for the calculated susceptibility of the Pr^{3+} ion in Pr-1:2:3-O_7 over the temperature range $100\leq T\leq300$ K.

The susceptibilities of Ho^{3+} and Nd^{3+} in R-1:2:3-O_7 have been calculated and fit in a similar manner. Analyzing these calculated values using the Curie Law we obtain $\mu_{\text{eff}}(Ho^{3+})=10.5\mu_B$ and $\mu_{\text{eff}}(Nd^{3+})=3.69\mu_B$. These results, together with the expected free-ion moments and experimentally determined values, are listed in Table V.

It can be seen, from the recent work on the relation of crystal-field parameters for tetragonal and for orthorhombic Ho-1:2:3-O_7,[49] that the symmetry axis to which our crystal-field calculation refers is the c axis of the crystal. Thus, the parallel contribution to the magnetic moment, $\mu_\parallel$ in our paper, can be related to the saturation moment along this c axis observed for the antiferromagnetically ordered phase.

We calculate a ground-state saturation moment $\mu_B=1.11\mu_B$ for Nd^{3+}. This moment compares with the experimentally determined value of $1.07\mu_B$,[51,52] which

TABLE V. A comparison of our calculated effective magnetic moments, μ_{eff}(calc), for Ho^{3+}, Nd^{3+}, and Pr^{3+} in R-1:2:3-O_7 with the expected free-ion values, μ_{eff}(FI), and with those obtained experimentally, μ_{eff}(expt). All values are in units of μ_B.

Compound	μ_{eff}(calc)	μ_{eff}(FI)	μ_{eff}(expt)	Ref.
Ho-1:2:3-O_7	10.5	10.61	10.2(3)	40, This work
Nd-1:2:3-O_7	3.69	3.62	3.57	50, This work
Pr-1:2:3-O_7	2.83	3.58	2.84(2)	19, This work

orders along the crystallographic c direction. Li *et al.*[7] studied the Pr analog by neutron diffraction. They observed two new diffraction peaks below 17 K which they attributed to magnetic diffraction peaks resulting from a long-range magnetic ordering of the Pr sublattice. From the intensities of these peaks, they determined a ground-state saturation moment for Pr^{3+} of $0.74\mu_B$. The crystal-field calculations presented here yield a vanishing ground-state moment on Pr because they completely ignore interactions between f electrons on different atoms. These intersite interactions produce the magnetic ordering, which is expected to result in a renormalization below T_N of the three lowest-lying, single-site, crystal-field energy states. This type of interaction is discussed in some detail elsewhere.[45]

DISCUSSION

The inelastic neutron scattering spectrum of the superconductor Nd-1:2:3-O_7 ($T_c = 92$ K), obtained at 15 K, exhibits four sharp, well-defined peaks which are attributed to crystal-field transitions. Spectra obtained under similar conditions for Pr-1:2:3-O_7, the nonsuperconducting analog of the Nd compound, show no evidence of any sharp, well-defined features. Furthermore, the neutron inelastic spectrum of the crystal-field states of Pr^{3+} in this compound is significantly different from that obtained for Pr^{3+} in a similar oxide environment, i.e., $PrScO_3$, where sharp, well-defined lines are observed.[53] $PrScO_3$ is a good comparison to Pr-1:2:3-O_7 because the perovskite environments of these two compounds are similar. However, unlike Pr-1:2:3-O_7, there are no free electrons (Sc^{3+} is a d^0 ion) with which the Pr f states can interact. Therefore, the large damping of crystal-field transitions in Pr-1:2:3-O_7 relative to the superconducting Nd-1:2:3-O_7 and the insulating $PrScO_3$ suggests an interaction between the Pr f electrons and the CuO electrons in Pr-1:2:3-O_7. This type of damping of magnetic scattering intensities in the R-1:2:3-O_7 series is unique to R = Pr—the only rare-earth member of this series which is not superconducting. The presence of this type of interaction is supported by the relatively high magnetic ordering temperature (T_N) observed for the Pr moments,[6,7] and suggests that this interaction is peculiar to Pr-1:2:3-O_7, and possibly also to Cm-1:2:3-O_7.

Despite the presence of an apparent electronic interaction of the Pr f moments with their environment, we have analyzed our results in terms of a single, isolated-ion crystal-field model. We have used cyrstal-field parameters obtained from the assignment of the magnetic transitions of Ho^{3+} in Ho-1:2:3-O_7 (Ref. 32) as the basis of our analysis. The method of analysis utilized here can be expected to result in crystal-field parameters that vary continuously from one rare-earth element to the next.[31,42] By applying a simple scaling procedure to the Ho^{3+} crystal-field parameters, we have obtained good assignments of our data for Nd^{3+} and for Pr^{3+} in R-1:2:3-O_7. A comparison of these predicted energy levels with the experimental spectra allows the assignment of the observed peaks. This comparison is particularly helpful for Pr-1:2:3-O_7 at lower energy ($E < 40$ meV), where the scaling predicts three energy levels. A fit based on these assignments results in a slight adjustment of the scaled parameters for Nd^{3+} and Pr^{3+} and a good representation of the positions and intensities of the observed peaks, as shown in Figs. 1 and 2.

$NdBa_2Cu_3O_7$

The calculated inelastic neutron scattering spectra of Nd-1:2:3-O_7 agree very well with experiment, as demonstrated in Fig. 1. Both the calculated line positions, and their intensities, reproduce well the experimental spectra. The linewidths used for the calculated crystal-field peaks represent essentially the instrumental resolution. The magnitude of the overall Nd^{3+} ground-state splitting resulting from our crystal field is much larger than that which would result from the previously determined energy level scheme.[36,37] In fact, we see no evidence for several of the low-lying transitions previously assigned, and we report the transition at 117 meV for the first time. These findings clearly show the importance of applying the method of scaling in situations of this type. The effective moment for Nd^{3+}, as well as for Ho^{3+} in R-1:2:3-O_7, calculated from our crystal-field scheme, are very close to the corresponding experimental values.[40,50] These results compare well with the free-ion values for these ions, as indicated in Table V. The saturation moment of $1.1\mu_B$ obtained for Nd^{3+} agrees very well with the $1.0\mu_B$ determined experimentally.[51,52] This result provides strong corroborating evidence that we have correctly analyzed the effect of the crystal field, since relatively small changes in the wave-function mixing can have large effects on the magnetic properties of the calculated ground state.

$PrBa_2Cu_3O_7$

A comparison of the calculated and experimental crystal-field spectra is more difficult for Pr^{3+}. As can be seen from Fig. 2, the lines are significantly broader than the instrumental resolution, and are of relatively weak intensity. Small phonon features, which do not significantly affect the Nd^{3+} spectra, become dominant features in the Pr case. Therefore, in order to compare experiment with calculation, it is necessary to estimate the nonmagnetic background which arises from this nuclear (phonon) scattering. Y-1:2:3-O_7 data can serve only as a rough estimate of the background, because of the differences in both the scattering lengths between Pr and Y, and in the phonon modes around 35 meV. Based on the Q-dependence studies of the intensity in the low-energy region [see Fig. 2(a)], we conclude that the excess intensity below about 10 meV is of magnetic origin. This conclusion is supported by other workers.[6,7] Our crystal-field analysis at 15 K, in the 0–10-meV region, shows that there are three crystal-field transitions corresponding to two excitations from the ground state to the first two excited states, and one from the first excited state to the second excited state (see Table IV). By choosing an intrinsic width of about 3.8 meV for the crystal-field peaks, folded into the instrumental resolution, we

obtain a calculated spectrum in good agreement with the data. A more detailed analysis of the low-energy magnetic spectra of Pr-1:2:3-O_7, including the data published by other workers, has been given elsewhere.[45] In the analysis of the high-energy region [see Fig. 2(c)] we use a background [see Fig. 2(b)] which underestimates the phonon contributions in the $10 \leq E \leq 40$-meV region. Comparing a variety of spectra, taken at different energies and scattering angles, including those obtained from Y-1:2:3-O_7 under similar conditions, has convinced us that the scattering intensity in the $15 \leq E \leq 40$-meV range is not of magnetic origin. In spite of the large uncertainty in the background, the overall calculated magnetic spectrum of Pr^{3+} is seen to agree well with experiment as shown in Fig. 2(c).

The parameters derived from the fits, in Table I, reveal that the crystal field at the R site is predominantly cubic. The three lowest crystal-field levels for Pr^{3+} are degenerate in cubic symmetry. The largest B's, (B_0^4, B_0^6, B_4^4, and B_4^6) are the cubic terms, and are well behaved during the fitting procedure. The splitting of these three levels, and their relative energies, is determined by the five small, noncubic terms. These noncubic crystal-field parameters, which account for the small deviation from cubic symmetry are highly correlated, and not well determined by the fitting procedure. In fact, the order of the lowest-lying energy levels is sensitive to the small noncubic term and therefore the transition strengths, listed in Table IV, may change markedly with slight changes in the noncubic part of the crystal field. In order to more accurately determine both the splittings of these low-lying states, and to further refine the calculated transition strengths, more experimental data, particularly from single-crystal measurements, are necessary to improve our model. We further refine this aspect of the work elsewhere.[45]

The energy levels and eigenvectors determined for the f element in this crystal field are used in turn to calculate the corresponding magnetic susceptibilities as a function of temperature for comparison with the experimental data. The comparison, shown in Fig. 3, is particularly illuminating for Pr-1:2:3-O_7 because the effective moment deduced from observations has been regarded as anomalously low for a Pr^{3+} ion. This low value has been used to argue for "mixed-valent" behavior of Pr in Pr-1:2:3-O_7. Our calculated effective moment, based on a normal trivalent Pr ion, has a value of $2.83\mu_B$, close to our experimental effective moment of $2.84\mu_B$. These values are, in turn, quite similar to other published experimental results.[12–19]

Fitting the calculated magnetic susceptibility over the temperature range of 100–300 K to the Curie Law yields a value of the temperature-independent paramagnetic (TIP) susceptibility of $\chi_0^{\rm Pr}=1.21\times10^{-3}$ emu/mol for Pr^{3+}. We find an experimental value of $\chi_0^{\rm expt}=2.18\times10^{-3}$ emu/mol (or 2.33×10^{-3} emu/mol after the standard diamagnetic correction) for Pr-1:2:3-O_7 determined over the same energy range. Our calculated value of the TIP includes only the contribution from Pr^{3+}, therefore it is tempting to attribute the constant difference between the calculated and observed TIP to contributions from the rest of the lattice, which are ignored in our calculation. This difference $\Delta\chi_0=0.97\times10^{-3}$ emu/mol, has been added to $\chi_0^{\rm Pr}$ to give the "calculated" points in Fig. 3, which then include contributions from the entire lattice. An independent estimate of these contributions could, in principal, be obtained from the available literature values of $\chi_0^{\rm Expt}$ for Y-1:2:3-O_7. These values are generally in the range of 0.33×10^{-3} emu/mol.[54] However, it has been found that the χ_0 for Y-1:2:3-O_x is significantly dependent on the exact oxygen stoichometry.[54] Furthermore, the dependence of χ_0 on lattice constants, which change with rare-earth substitution, has not been analyzed. Therefore, it is not possible at present to make a reliable, independent estimate of the contribution to $\Delta\chi_0$ from the rest of the lattice.

The reduced value for the effective moment of Pr^{3+} in Pr-1:2:3-O_7, the unexpected linearity of the Curie plot, and the small χ_0 contribution to the susceptibility, can all be understood in terms of a rather unusual splitting pattern for the lowest electronic energy levels. Normally in this low-symmetry site, the $J=4$ states of the ^3H multiplet for Pr^{3+} should be split into nine distinct, nondegenerate energy levels. This complete lifting of degeneracies occurs here, but the pattern of the splittings is rather unusual. According to the crystal-field calculation, the first two excited states ($E<5$ meV) are energetically very close to the ground state, with the other excited states at much higher energies ($E>40$ meV). This pattern of splittings means that over the energy range in which most of the susceptibility data were collected (about 50–300 K), the system behaves as though it has three isolated, low-lying energy levels, that contribute to the dominant temperature-dependent magnetic susceptibility. The remaining energy levels are high enough in energy, and have small enough magnetic matrix elements, that they do not contribute significantly to the calculated susceptibility over the temperature range of interest. Although the true, nondegenerate ground state has no magnetic moment, the first two excited states are well populated in the temperature range of interest. Since there are nonzero magnetic matrix elements connecting these states Pr^{3+} behaves as though it has a nonzero ground-state magnetic moment. (This situation can be treated in the van Vleck formula for χ by expanding the Boltzmann exponential factors, through the linear term, for the three lowest energy levels and then completing the sum over these three energy levels.) The result is that the susceptibility appears to obey the simple Curie Law, with a reduced effective moment.

As previously discussed, a renormalization of our calculated low-energy states is expected below the long-range magnetic ordering temperature of 17 K for Pr^{3+}. This interaction is not included in our calculations, and therefore we cannot determine a saturation magnetic moment for Pr^{3+} to compare with experiment.

We find entirely satisfactory agreement of the calculated and experimentally determined parameters associated with the magnetic behavior of Pr ions in the paramagnetic phase of Pr-1:2:3-O_7. We want to stress that the interpretation of the data outlined above is based strictly on a standard crystal-field treatment of the f^2 configuration

for Pr^{3+} in *mmm* site symmetry. The susceptibility has been calculated directly from these crystal-field eigenfunctions and eigenvalues using a standard van Vleck formalism. We have not had to include any "orbital reduction factor k" that is sometimes invoked to improve the agreement between the calculated and experimental values.[55] The good agreement of standard crystal-field calculations with the observed magnetic properties for Pr-1:2:3-O_7 proves that it is not necessary to invoke "mixed valent" behavior to account for the low effective moment on the Pr ions, nor is it necessary to have Pr^{4+} to account for the nonzero ground-state moment found from elastic neutron scattering on the ordered state.[7]

The foregoing analysis of magnetic properties is fully consistent with our cluster calculations,[29] but provides much more detailed information about the lowest energy states than do the cluster calculations. Mulliken analyses on Pr, Nd, Ho, and Cm, confirm that the f-element ion is trivalent in each case.[29] The agreement of the calculated and experimental magnetic features seems to indicate that the static magnetic properties of Pr are not noticeably influenced by the unusual admixing of wave functions, seen in the Mulliken analyses, between the Pr or Cm f states and the Cu d states. Nevertheless, the absence of superconductivity for Pr-1:2:3-O_7 and Cm-1:2:3-O_7 appears to be caused by interactions associated with these unusual mixings of wave functions, rather than any "mixed-valent behavior."

The observed magnetic properties of Pr-1:2:3-O_7 have been deduced from a knowledge of the observed locations and expected behaviors of the low-lying electronic states for the f^2 configuration of an essentially trivalent Pr ion. A simple model involving the presence of only Pr^{4+} is clearly ruled out by the neutron inelastic data alone, since Pr^{4+} has an f^1 configuration, with a $^2F_{5/2}$ ground term, and therefore only three expected magnetic transitions over the energy range probed by the experiment. Instead, seven transitions can be assigned to the observed spectra, compared to the eight possible transitions expected for a Pr^{3+}, $^3H_4$ ground term. Furthermore, the reconcilliation of magnetic and trivalent electronic properties eliminates the major reason for giving serious considerations to any "mixed-valence" description of Pr in this compound. Interpretation of the magnetic data is now in agreement with the generally accepted interpretation of a wide variety of other microscopic and macroscopic properties of Pr-1:2:3-O_7.

While a simple crystal-field analysis can explain the spectroscopic and magnetic features of Pr^{3+} in Pr-1:2:3-O_7, it does not explain the absence of superconductivity in this, or the Cm analog. In fact, both the appearance of the inelastic spectrum, which shows broadened peaks, as well as our calculations,[29] are consistent with an interaction of the f electrons with the conduction electrons. It should be noted that this interaction involves the peripheral f-electron density, primarily in the spatially extended region (tail of the radial distribution function) of the wave functions. The magnetic measurements and crystal-field analysis, on the other hand, reflect the behavior of the bulk of the electron density, which is spatially closer to the Pr nucleus. Since the latter represents the greater part of the electron density, it is not surprising that the localized calculations can well represent the magnetic behavior. Other experiments, which would be much more sensitive to details of the Pr-electron density farther from the nucleus are necessary to probe details of this interaction. We do conclude from our analysis that the interaction of the f electrons with their environment is subtle, and not a substantial removal of charge from the Pr atom of the type described as "mixed valency."

The bulk of the evidence points toward trivalent Pr. We believe that the results of our study essentially eliminate from further consideration any mechanism for the suppression of superconductivity in Pr-1:2:3-O_7 that requires a significant charge transfer from the rare-earth ion to the CuO planes. Instead, a likely mechanism for this suppression of superconductivity involves a more subtle magnetic interaction. Evidence of this subtle interaction has been previously seen in inelastic neutron scattering data,[28] specific heat measurements,[7] trends in rare-earth magnetic ordering,[7–9] and critical-field experiments.[5] The specifics of this interaction have yet to be explained in detail, although a full understanding of the nonsuperconducting members of the R-1:2:3-O_7 series may well lead to important insights into the mechanisms responsible for superconductivity itself.

CONCLUSIONS

Inelastic neutron scattering data have been obtained in Nd-1:2:3-O_7 and Pr-1:2:3-O_7. With only minor modifications to the published crystal-field parameters of Ho-1:2:3-O_7,[32] a simple scaling procedure has been used to assign the transitions observed for Nd^{3+} and Pr^{3+}. These transitions have been fitted to obtain a set of eigenfunctions and eigenvalues for Nd and Pr in this crystal environment. The peak energies and their relative intensities calculated from the fitted parameters agree well with the experimental data. The calculated paramagnetic susceptibilities also agree well with experiment. This is particularly significant for Pr-1:2:3-O_7, since its reduced experimental susceptibility has been used to argue mixed valence for Pr in this system.

Unlike the spectrum obtained from the Nd compound, the inelastic spectrum obtained from Pr-1:2:3-O_7 shows only broad, low-intensity peaks. However, using a simple crystal-field model, based on Pr^{3+}, and initial parameters scaled from Ho^{3+} and Nd^{3+}, we were able to fit both the energies and relative intensities of the observed peaks. The eigenfunctions and eigenvalues obtained from this procedure were then used to calculate an effective magnetic moment of $2.83\mu_B$ for Pr^{3+}, very close to the observed value.

We have demonstrated that the reduced magnetic susceptibility can be explained entirely in terms of a crystal-field splitting of the $^3H_4$ Pr^{3+} ground term. There is no need to invoke "mixed valence" behavior of the Pr ion in order to account for the reduced magnetic moment. However, this simple explanation of the magnetic properties does not explain the broadness of the peaks observed

for the inelastic magnetic transitions. Further experiments are necessary to determine if this broadening is the result of dynamic, f-electron–Cu-spin interactions, or whether there is a static effect, such as a slight Pr f-orbital hybridization, which results in the significant line broadening, even at low temperatures. Either of these interactions could be sufficient to inhibit superconductivity in Pr-1:2:3-O_7.

ACKNOWLEDGMENTS

We wish to thank B. D. Dunlap and H. B. Radousky for helpful discussions. This work is supported by the U.S. DOE, Basic Energy Sciences-Chemical and Materials Sciences, and has benefited from the use of the Intense Pulsed Neutron Source at Argonne National Laboratory, all under Contract No. W-31-109-ENG-38.

[1]P. H. Hor, R. L. Meng, Y. Q. Wang, L Gao, Z. J. Huang, J. Bechtold, K. Forster, and C. W. Chu, Phys. Rev. Lett. **58**, 1891 (1987).

[2]J. O. Willis, Z. Fisk, J. D. Thompson, S.-W. Cheong, R. M. Aikin, J. L. Smith, and E. Zirngiebl, J. Magn. Magn. Mater. **67**, L139 (1987).

[3]D. W. Murphy, S. Sunshine, R. B. van Dover, R. J. Cava, B. Batlogg, S. M. Zahurak, and L. F. Schneemeyer, Phys. Rev. Lett. **58**, 1888 (1987).

[4]L. Soderholm, K. Zhang, D. G. Hinks, M. A. Beno, J. D. Jorgensen, C. U. Segre, and Ivan K. Schuller, Nature (London) **328**, 604 (1987).

[5]J. L. Peng, P. Klavins, R. N. Shelton, H. B. Radousky, P. A. Hahn, and L. Bernardez, Phys. Rev. B **40**, 4517 (1989).

[6]E. Gering, B. Renker, F. Gompf, D. Ewert, H. Schmidt, R. Agrens, M. Bonnet, and A. Dianoux, Physica C **153-155**, 184 (1988).

[7]W.-H. Li, J. W. Lynn, S. Skanthakumar, T. W. Clinton, A. Kebede, C.-S. Jee, J. E. Crow, and T. Mihasisin, Phys. Rev. B **40**, 5300 (1989); S. Skanthakumar, W.-H. Li, J. W. Lynn, A. Kebede, J. E. Crow, and T. Mihalisin, Physica B **163**, 239 (1990).

[8]S. E. Brown, J. D. Thompson, J. O. Willis, R. M. Aikin, E. Zirngiebl, J. L. Smith, Z. Fisk, and R. B. Schwarz, Phys. Rev. B **36**, 2298 (1987).

[9]A. P. Ramirez, L. F. Schneemeyer, and J. V. Waszcak, Phys. Rev. B **36**, 7145 (1987).

[10]L. Soderholm, G. L. Goodman, U. Welp, C. W. Williams, and J. Bolender, Physica C **161**, 252 (1989).

[11]D. G. Hinks, B. Dabrowski, K. Zhang, C. U. Segre, J. D. Jorgensen, L. Soderholm, and M. A. Beno, Mat. Res. Soc. Symp. Proc. **99**, 9 (1988).

[12]E. Moran, U. Amodor, M. Barahona, M. A. Alario-France, A. Vegas, and J. Rodriguez-Carvajal, Solid State Commun. **67**, 369 (1988).

[13]Y. Dalichaouch, M. S. Torikachvili, E. A. Early, B. W. Lee, C. L. Seaman, K. N. Yang, H. Zhou, and M. B. Maple, Solid State Commun. **65**, 1001 (1988).

[14]D. B. Mitzi, P. T. Feffer, J. M. Newsam, K. J. Webb, P. Klavins, A. J. Jacobson, and A. Kapitulnik, Phys. Rev. B **38**, 6667 (1988).

[15]Bin Okai, Michikazu Kosuge, Hiroshi Nozaki, Koh Takahashi, and Masatsune Ohta, Jpn. J. Appl. Phys. **27**, L41 (1988).

[16]Azusa Matsuda, Kyoichi Kinoshita, Takao Ishii, Hiroyuki Shibata, Takao Watanabe, and Tomoski Yamada, Phys. Rev. B **38**, 2910 (1988); Azusa Matsuda, Kyoichi Kinoshita, Takao Ishii, Hiroyuki Shibata, Takao Watanabe, and Tomoski Yamada, *Advances in Superconductivity* (Springer, Tokyo, 1989), p. 191.

[17]Cha-Soo Jee, A. Kebede, T. Yuen, S. H. Bloom, M. V. Kuric, J. E. Crow, T. Mihalisin, and P. Schlottmann, J. Magn. Magn. Mater. **76&77**, 617 (1989).

[18]A. Kebede, Chan-Soo Jee, D. Nichols, M. V. Kuric, J. E. Crow, R. P. Guertin, T. Mihalisin, G. H. Myer, I. Perez, R. E. Salomon, and P. Schlottmann, J. Magn. Magn. Mater. **76&77**, 619 (1989).

[19]L. Soderholm and G. L. Goodman, J. Solid State Chem. **81**, 121 (1989).

[20]J. S. Kang, J. W. Allen, Z. X. Shen, W. P. Ellis, J. J. Yeh, B. W. Lee, M. B. Maple, W. E. Spicer, and I. Lindau, J. Less Common Metals **148**, 121 (1989).

[21]U. Neukrich, C. T. Simmons, P. Slakeczek, C. Laubschat, O. Strebel, G. Kaindl, and D. D. Sarma, Europhys. Lett. **5**, 567 (1988).

[22]E. E. Alp, L. Soderholm, G. K. Shenoy, D. G. Hinks, B. W. Veal, and P. A. Montano, Physica B **150**, 74 (1988).

[23]H. B. Radousky, K. F. McCarty, J. L. Peng, and R. N. Shelton, Phys. Rev. B **39**, 12 383 (1989).

[24]J. D. Jorgensen, M. A. Beno, D. G. Hinks, L. Soderholm, K. J. Volin, R. L. Hitterman, J. D. Grace, Ivan K. Schuller, C. U. Segre, K. Zhang, and M. S. Kleefisch, Phys. Rev. B **36**, 3608 (1987).

[25]D. C. Johnston, A. J. Jacobson, J. M. Newsam, J. T. Lewandowski, D. P. Goshorn, D. Xie, and W. B. Yelon, in *Chemistry of High Temperature Superconductors,* (edited by David Nelson, M. S. Whittingham, and Thomas F. George) ACS Symposium Series 351 (Amer. Chem. Soc.., Washington, D.C., 1987), p. 136.

[26]A. Kebede, C. S. Jee, J. Schwegler, J. E. Crow, T. Mihalisin, G. H. Myer, R. E. Salomon, P. Schlottmann, M. V. Kuric, S. H. Bloom, and R. P. Guertin, Phys. Rev. B **40**, 4453 (1989).

[27]G. Y. Guo and W. M. Temmerman, Phys. Rev. B **41**, 6372 (1990).

[28]L. Soderholm, C.-K. Loong, G. L. Goodman, U. Welp, J. Bolender, and C. W. Williams, Physica B **163**, 655 (1990).

[29]G. L. Goodman and L. Soderholm, Physica C **171**, 528 (1990).

[30]G. L. Goodman, D. E. Ellis, E. E. Alp, and L. Soderholm, J. Chem. Phys. **91**, 2983 (1989).

[31]W. T. Carnall, G. L. Goodman, K. Rajnak, and R. S. Rana (unpublished).

[32]A. Furrer, P. Bruesch, and P. Unternahrer, Phys. Rev. B **38**, 4616 (1988).

[33]A. Furrer, P. Bruesch, and P. Unternahrer, Solid State Commun. **67**, 69 (1988).

[34]H. M. Rietveld, J. Appl. Crystallogr. **2**, 65 (1969).

[35]M. A. Beno, L. Soderholm, D. W. Capone II, D. G. Hinks, J. D. Jorgensen, Ivan K. Schuller, C. U. Segre, K. Zhang, and J. D. Grace, Appl. Phys. Lett. **51**, 57 (1987).

[36]P. Allenspach, A. Furrer, P. Bruesch, and P. Unternahrer, Physica B **156&157**, 864 (1989).

[37]U. Walter, E. Holland-Moritz, A. Serving, A. Erle, H. Schmidt, and E. Zirngiebl, Physica C **153-155**, 170 (1988).

[38]C.-K. Loong, G. L. Goodman, L. Soderholm, B. Dabrowski,

and D. G. Hinks, J. Appl. Phys. **67**, 4536 (1990).
[39]D. McK. Paul, B. D. Rainford, R. Osborn, A. T. Boothroyd, and L. Caver (unpublished).
[40]B. D. Dunlap, M. Slaski, D. G. Hinks, L. Soderholm, M. Beno, K. Zhang, C. Segre, G. W. Crabtree, W. K. Kwok, S. K. Malik, Ivan K. Schuller, J. D. Jorgensen, and Z. Sungaila, J. Magn. Magn. Mater. **68**, L139 (1987).
[41]H. M. Crosswhite and H. Crosswhite, J. Opt. Soc. Am. B **1**, 246 (1984).
[42]W. T. Carnall, G. L. Goodman, K. Rajnak, and R. S. Rana, J. Chem. Phys. **90**, 3443 (1989).
[43]K. W. H. Stevens, Proc. Phys. Soc. A **65**, 209 (1952).
[44]A. J. Kassman, J. Chem. Phys. **53**, 4118 (1970).
[45]G. L. Goodman, C.-K. Loong, and L. Soderholm, J. Phys. Condens. Matter (to be published).
[46]A. J. Freeman and R. E. Watson, Phys. Rev. **127**, 2058 (1962).
[47]J. H. van Vleck, *The Theory of Electric and Magnetic Susceptibilities* (Oxford University Press, London, 1932).
[48]R. M. White, *Quantum Theory of Magnetism,* Springer Series in Solid-State Sciences, Vol. 32 (Springer, New York, 1983).
[49]P. Allenspach, A. Furrer, P. Bruesch, R. Marsolais, and P. Unternahrer, Physica C **157**, 58 (1989).
[50]S. Chittipeddi, A. J. Epstein, Y. Song, J. R. Gaines, W. E. Farneth, and E. M. McCarron III, Synth. Metals **29**, F651 (1989).
[51]P. Fischer, B. Schmid, P. Bruesch, F. Stucki, and P. Unternahrer, Z. Phys. B **74**, 183 (1989).
[52]K. N. Yang, J. M. Ferreira, B. W. Lee, M. B. Maple, W.-H. Li, J. W. Lynn, and R. W. Erwin, Phys. Rev. B **40**, 10 963 (1989).
[53]L. Soderholm, G. L. Goodman, and C.-K. Loong, J. Appl. Phys. **67**, 5067 (1990).
[54]D. C. Johnston, S. K. Sinha, A. J. Jacobson, and J. M. Newsam, Physica C **153-155**, 572 (1988).
[55]J. S. Griffith, *The Theory of Transition-Metal Ions* (Cambridge University Press, London, 1961).